Published in final edited form as:
Int J Cancer. 2014 June 15; 134(12): 2853–2864. doi:10.1002/ijc.28622.

Subpopulations of Myeloid-Derived Suppressor Cells (MDSC) impair T cell responses through independent nitric oxide-related pathways

Patrick L. Raber[1,2], **Paul Thevenot**[2], **Rosa Sierra**[2], **Dorota Wyczechowska**[2], **Daniel Halle**[2], **Maria E. Ramirez**[2], **Augusto Ochoa**[2,3], **Matthew Fletcher**[2,3], **Cruz Velasco**[2], **Anna Wilk**[2], **Krzysztof Reiss**[2], and **Paulo C. Rodriguez**[1,2]

[1]Department of Microbiology, Immunology and Parasitology, Louisiana State University Health Sciences Center, New Orleans, LA

[2]Stanley S. Scott Cancer Center, Louisiana State University Health Sciences Center, New Orleans, LA

[3]Department of Pediatrics, Louisiana State University Health Sciences Center

Abstract

The accumulation of myeloid-derived suppressor cells (MDSC) in tumor-bearing hosts is a hallmark of malignancy-associated inflammation and a major mediator for the induction of T cell suppression in cancer. MDSC can be divided phenotypically into granulocytic (G-MDSC) and monocytic (Mo-MDSC) subgroups. Several mechanisms mediate the induction of T cell anergy by MDSC; however, the specific role of these pathways in the inhibitory activity of MDSC subpopulations remains unclear. Therefore, we aimed to determine the effector mechanisms by which subsets of tumor-infiltrating MDSC block T cell function. We found that G-MDSC had a higher ability to impair proliferation and expression of effector molecules in activated T cells, as compared to Mo-MDSC. Interestingly, both MDSC subgroups inhibited T cells through nitric oxide (NO)-related pathways, but expressed different effector inhibitory mechanisms. Specifically, G-MDSC impaired T cells through the production of peroxynitrites (PNT), while Mo-MDSC suppressed by the release of NO. The production of PNT in G-MDSC depended on the expression of $gp91^{phox}$ and endothelial NO synthase (eNOS), while inducible NO synthase (iNOS) mediated the generation of NO in Mo-MDSC. Deletion of eNOS and $gp91^{phox}$ or scavenging of PNT blocked the suppressive function of G-MDSC and induced anti-tumoral effects, without altering Mo-MDSC inhibitory activity. Furthermore, NO-scavenging or iNOS knockdown prevented Mo-MDSC function, but did not affect PNT production or suppression by G-MDSC. These results suggest that MDSC subpopulations utilize independent effector mechanisms to regulate T cell function. Inhibition of these pathways is expected to specifically block MDSC subsets and overcome immune suppression in cancer.

Introduction

The increase of different mediators of chronic inflammation promotes the development, growth, and metastasis of malignant tumors in part through the inhibition of protective immune responses.[1] A characteristic of cancer-linked inflammation is the accumulation of myeloid-derived suppressor cells (MDSC), a heterogeneous population of immature myeloid

Correspondence should be addressed to: Paulo C. Rodriguez, PhD. Stanley S. Scott Cancer Center, Louisiana Cancer Research Consortium (LCRC), Louisiana State University Health Sciences Center. 1700 Tulane Ave Room 910, New Orleans, LA, 70112, USA, Tel: (504) 210-3324; prodri1@lsuhsc.edu.

cells that potently inhibit the function of T, NK, and dendritic cells.[2,3] MDSC accumulate in tumors and other tissues as the result of the elevated levels of pro-inflammatory mediators produced by the malignant cells and the tumor stroma.[4] A similar link between inflammation, high numbers of MDSC, and immune suppression also occurs in chronic infectious diseases, sepsis, trauma, and autoimmunity.[5] In mice, MDSC are characterized by the expression of CD11b and Gr-1.[6] Among this group of cells, MDSC are phenotypically divided into granulocytic (G-MDSC, $CD11b^{+}Ly6C^{LOW}$ $Ly6G^{HIGH}$) and monocytic (Mo-MDSC, $CD11b^{+}$ $Ly6C^{HIGH}$ $Ly6G^{NEG}$) subpopulations.[6]

The most studied function attributed to MDSC in tumor-bearing hosts is their ability to suppress T cell responses. This inhibitory function is linked to several suppressive pathways including the metabolism of the amino acid arginine by arginase I and inducible nitric oxide synthase (iNOS), leading to arginine starvation[7–9] and the production of nitric oxide (NO)[10,11], respectively. In addition, MDSC inhibit T cell responses through the generation of reactive oxygen species (ROS) initiated by NADPH oxidase 2 ($gp91^{phox}$)[12,13], and the combination of NO and superoxide anion (O_2^{-}), resulting in the formation of peroxynitrites (PNT).[14–16] While these mechanisms are closely linked to the suppressive ability of MDSC as a whole, it remains unclear the specific role of these pathways in the T cell suppression induced by G-MDSC and Mo-MDSC.

Production of NO and PNT by MDSC leads to T cell tolerance through still unclear mechanisms. High levels of NO and PNT arrested cellular protein synthesis, decreased cellular defense against DNA damage, and blocked cell proliferation.[10,17,18] PNT nitrosylates sulfate and thiol residues, thereby promoting or inhibiting protein function.[19] Nitrosylation of the T cell receptor or major histocompatibility antigens induced by MDSC-linked PNT impaired antigen presentation and recognition by $CD8^{+}$ T cells.[14,16] In addition, PNT inhibited T cell chemotaxis into tumors and promoted T cell apoptosis.[18,20,21] The significance of the production of PNT and NO in tumor-induced tolerance was suggested by the increased presence of nitrotyrosine residues in human cancers including prostate, colon, and liver;[20,22] and the reversed immune suppression induced by PNT scavengers.[23,24] Although the effect of NO and PNT in the immune regulatory function induced by MDSC is established, it continues unclear the specific role of these reactive agents in the function of MDSC subsets.

In this study, we aimed to characterize the suppressive pathways by which subpopulations of tumor-infiltrating MDSC block T cell function. A higher capacity to impair T cell responses was observed in G-MDSC, as compared to Mo-MDSC. In addition, we found that both MDSC subpopulations depended on NO-related pathways for their suppression of T cell responses. However, MDSC subsets used independent effector mechanisms to accomplish their negative regulation of T cells. G-MDSC produced PNT through $gp91^{phox}$ and endothelial NO synthase (eNOS), while Mo-MDSC primarily released NO through iNOS. Accordingly, inhibition or knockdown of $gp91^{phox}$ and eNOS prevented PNT production and suppression in G-MDSC and led to anti-tumor effects, without affecting Mo-MDSC activity. In contrast, targeting of iNOS inhibited growth of tumors having high numbers of Mo-MDSC and impaired suppression in Mo-MDSC, but not in G-MDSC. Taken together, our data indicates the independent suppressive pathways by which tumor-infiltrating MDSC-subpopulations impair T cell function. These findings may enable the development of potential therapies to specifically block particular MDSC subpopulations in cancer and other diseases characterized by the accumulation of MDSC subsets and T cell dysfunction.

Materials and Methods

Animals and Cell Lines

Lewis lung carcinoma (3LL), MCA-38 colon adenocarcinoma cell, EL-4 thymoma, and B16 (F1) melanoma (American Type Culture Collection, Manassas, VA) were maintained in RPMI 1640 (Lonza-Biowhittaker, Walkerville, MD) supplemented with 10% fetal calf serum (Hyclone, Logan, UT), 25 mM Hepes (Invitrogen, Life Technologies, Grand Island, NY), 4 mM L-glutamine (Invitrogen, Life Technologies), and 100 U/ml of penicillin, streptomycin (Invitrogen, Life Technologies). C57BL/6 mice (6 to 8-wk-old female) from Harlan (Indianapolis, IN), B6.129S-*Cybb*^{tm1Din}/J (gp91$^{phox-/-}$), B6.129P2-*Nos3*^{tm1Unc}/J (eNOS−/−), and B6.129P2-*Nos2*^{tm1Lau}/J (iNOS−/−) mice (The Jackson Laboratories, Bar Harbor, ME) were injected subcutaneously with 1×10^6 3LL, MCA-38, or EL-4 cells, or 1×10^5 B16 tumors. For *in vivo* experiments scavenging PNT and inhibiting NO synthases, 6 to 8 wk-old female C57BL6/J mice were subcutaneously injected with 1×10^6 3LL or MCA-38 cells and treated daily with 10 mg/kg Manganese (III) Tetrakis (4-Benzoic Acid) Porphyrin chloride (MnTBAP), 20 mg/kg L-N^6-(1-Iminoethyl) lysine dihydrochloride (L-NIL), or PBS vehicle. Tumor volume was determined using calipers and calculated using the formula [(small diameter)^2 × (large diameter) × 0.5]. All experiments using animals were approved by the LSU-IACUC and were performed following LSU animal care facility guidelines.

Antibodies and Reagents

Purified antibodies against CD3 (clone 145-2C11), CD28 (clone 37.51), arginase I (clone 19), eNOS/NOS Type III (clone 3), iNOS/NOS Type II (clone 54), and gp91^{phox} (clone 53) were obtained from Becton Dickinson Biosciences (BD Biosciences, San Jose, CA). Anti-granzyme B antibodies were obtained from Cell Signaling Technology (Danvers, MA) and eBioscience (clone NGZB). Anti-β-actin antibody (clone AC-74) was obtained from Sigma-Aldrich (St. Louis, MO). 3-Morpholinosydnonimine hydrochloride (SIN-1) was obtained from Sigma-Aldrich. PNT, N$^{\omega}$-hydroxy-nor-Arginine (NN), L-NG-Monomethylarginine (L-NMMA), D-NG-Monomethylarginine (D-NMMA), and MnTBAP were obtained from EMD Millipore (Calbiochem, Gibbstown, NJ).

Isolation of T cells and MDSC subsets

CD3$^+$ T cells were isolated from the spleen and lymph nodes of C57BL/6 mice using a T cell negative isolation kit (Life Technologies). Purity ranged between 95% and 99% as tested by flow cytometry. MDSC, G-MDSC, and Mo-MDSC were isolated from tumors previously digested with DNAse and Liberase (Roche USA, Branchburg, NJ) at 37°C for 1 hour, as previously described[25]. Briefly, total MDSC were isolated by positive selection using anti-Gr-1 antibodies (Stem Cell Technologies, Vancouver, BC, Canada); G-MDSC were initially labeled with anti-Ly6G-PE antibodies (BD Biosciences) and then selected using a PE positive isolation kit (Stem Cell Technologies); and Mo-MDSC were collected from G-MDSC depleted fractions using Ly6C-PE antibodies and PE positive isolation kit. Purity for each population ranged from 90%-99% as measured by flow cytometry.

Flow cytometry

For the intracellular detection of IFNγ by flow cytometry, the activated T cells were co-cultured with MDSC (ratio 1:1/2) for a period of 72 hours, after which T cells were isolated using negative selection kits (Life Technologies) and cultured (1×10^6/ml) in the presence of Golgi Plug reagent (Becton Dickinson), phorbol myristate acetate (PMA, 750ng/mL), and ionomycin (50μg/mL) for 6 hours. Then, T cells were stained with anti-CD3-PECy7, followed by intracellular staining of IFNγ (eBioscience, clone XMG1.2) using Cytofix/

Cytoperm™ Fixation/Permeabilization buffer (Becton Dickinson). Furthermore, intracellular expression of granzyme-B was achieved in T cells: MDSC co-cultures after staining of T cells with anti-CD3-APC, followed by intracellular detection of granzyme B (eBioscience, clone NGZB) using Cytofix/Cytoperm™ buffer. T cells were analyzed by FACS analysis using a Gallios flow cytometer (Beckman Coulter, Miami, FL) gating on $CD3^+$ cells to monitor the expression and percentage of T cells positive for IFNγ or granzyme B.

Western Blot

Cellular lysates were collected from tumor-infiltrating MDSC, G-MDSC, or Mo-MDSC from 3LL, MCA-38, and EL-4 tumors. Then, 30 micrograms of protein were electrophoresed in 8% TrisGlycine gels, transferred to PVDF membranes, and immunoblotted with antibodies against arginase I, iNOS, eNOS, $gp91^{phox}$, and β-actin (All used at 1:1000). For detection of granzyme B in T cells co-cultured with MDSC, the MDSC were removed by positive selection using anti-CD11b (EasySep STEMCELL technologies) and T cells (95–99% purity) used to collect protein extracts. Lysates were then electrophoresed in 12% TrisGlycine gels, transferred to PVDF membranes, and immunoblotted against granzyme B and β-actin (1:1000). Membrane-bound immune complexes were detected using ECL western blotting detection reagent (GE Healthcare).

Immunofluorescence

Total MDSC, as well as G-MDSC and Mo-MDSC subpopulations, were obtained by positive selection from tumor digests and adhered to slides by cytospin. Slides were then fixed in −20°C methanol for 10 minutes and blocked with 5% BSA in PBS. Slides were incubated overnight with primary antibodies against iNOS (1:100), eNOS (1:250), arginase I (1:50), and $gp91^{phox}$ (1:250) all from BD Biosciences. Alexa Fluor 594 goat anti-mouse secondary antibodies (Life Technologies) were applied at 1:250 for 1 hour followed by nuclear staining with DAPI. Images were captured at equal exposure. Quantification of number of voxel per cell for arginase I, $gp91^{phox}$, iNOS, and eNOS was achieved using the Mask analysis included in SlideBook5 software according to manufacturer recommendation (Intelligent Imaging Innovations Inc.)

T cell Proliferation Assay

T cell proliferation was measured using the intracellular dye Carboxyfluorescein succinimidyl ester (CFSE) (Molecular Probes, Life Technologies). T cells were labeled with 1 μM CFSE at 37°C for 15 minutes, followed by quenching in 10% FBS-RPMI 1640. Fluorescence was analyzed by FACS analysis using a Gallios flow cytometer. For T cell: MDSC co-cultures, 1×10^6 cells T cells were plated in wells bound with anti-CD3 and anti-CD28 antibodies (0.5 μg/ml each) and cultured with MDSC or MDSC subpopulations for 72 hours. Data is expressed as the percentage of T cells proliferating as determined by the dilution of CFSE fluorescence compared with non-activated T cells.

Measurement of Reactive oxygen species, Nitrite, and Peroxynitrite Production

Production of reactive oxygen species (ROS) was measured using 2',7'-dichlorodihydrofluorescein diacetate (DCFDA) (Molecular probes, Life Technologies). Nitrite production was quantified using standard Griess reagent (Molecular probes, Life Technologies). PNT production was measured by quantitating nitrotyrosine residues from lysates of tumor-derived MDSC, G-MDSC, and Mo-MDSC by Nitrotyrosine ELISA (EMD Millipore), according to the manufacturer's instructions.

Statistical Analysis

Statistical analyses were carried in SAS 9.3 (SAS Institute, Cary, NC). Tests were conducted at 5% significance level. Continuous data were checked for unequal variances with the Brown-Forsythe and Levene tests. Percentage data were arcsine transformed and further checked for unequal variances. Experimental groups differences of endpoints were assessed by ANOVA with the Satterthwaite correction for unequal variances using the MIXED procedure. Means comparisons were carried out with the Tukey procedure for all comparisons or with the Dunnet procedure for comparisons with the control group.

Results

MDSC subsets suppress T cell function through nitric oxide-related pathways

The specific mechanisms by which MDSC subpopulations impair T cell responses continue poorly characterized. Therefore, we compared the ability of MDSC subgroups from mice bearing 3LL or MCA-38 tumors to inhibit T cell function. In both tumor models, G-MDSC had a higher capacity to block T cell proliferation, as compared to Mo-MDSC (Fig. 1A). A similar effect was also observed in mice injected with tumors EL-4 and B16 (data not shown). We then tested the role of the metabolism of arginine in the regulatory function of MDSC subsets. The addition of the common NO synthase inhibitor, L-NMMA, but not the arginase inhibitor NN or the inactive NO synthase inhibitor D-NMMA, restored T cell proliferation and IFNγ production in cultures containing MDSC, G-MDSC, and Mo-MDSC (Fig. 1B–C). Moreover, the addition of L-NMMA, but not NN, into T: MDSC co-cultures rescued the expression of the effector molecule granzyme B in T cells (Fig. 1D and Suppl. Fig. 1A–B). To assess the relevance of these findings *in vivo*, we treated 3LL-bearing mice with the NO synthase inhibitor L-NIL and monitored tumor burden and MDSC subset activity. A decreased tumor growth was found in 3LL-bearing mice treated with L-NIL, as compared to those receiving PBS (Fig. 1E). Furthermore, a significant reduction in the ability of G-MDSC and Mo-MDSC to block T cell proliferation was observed in L-NIL-treated mice, as compared to MDSC subsets isolated from the tumor-bearing controls (Fig. 1F). These results suggest the major role of NO-related pathways in the T cell suppression induced by tumor-infiltrating MDSC subpopulations.

MDSC subsets express independent T cell suppressive effector mechanisms

To better understand the role of the NO production and the differential magnitude of T cell inhibition induced by MDSC subsets, we compared the expression of a panel of enzymes mediating MDSC suppressive activity. Using MDSC subpopulations collected from mice bearing 3LL, MCA-38, and EL-4 tumors, we found that G-MDSC preferentially expressed arginase I, NADPH oxidase $gp91^{phox}$, and eNOS, whereas Mo-MDSC displayed a higher expression of iNOS (Fig. 2A). This profile was validated using cytofluorescence experiments, finding a similar distribution of these suppressive enzymes (Fig. 2B and Suppl. Fig. 2). Additional results showed a higher production of reactive oxygen species in G-MDSC, as compared to Mo-MDSC (Suppl. Fig. 3). Then, we investigated whether the differential protein profiles in MDSC subpopulations affected the production of NO-linked effector molecules NO and PNT. A higher production of PNT was detected in G-MDSC isolated from 3LL, MCA-38, and EL-4 tumors, while Mo-MDSC preferentially released higher levels of NO (Fig. 2C–D). Furthermore, treatment of activated T cells with PNT or NO donor Sin-1 reproduced the effects induced by MDSC subsets, as they inhibited T cell proliferation and prevented the expression of IFNγ and granzyme B in a dose-dependent manner (Suppl. Fig. 4).

To test whether MDSC subpopulations use independent NO-related mechanisms to suppress T cell responses, we used MnTBAP, a compound previously shown to preferentially

scavenge PNT.[26] In addition, we used PTIO, a NO radical scavenger that reacts with NO, without affecting PNT production.[27] The addition of MnTBAP partially rescued the proliferation of T cells co-cultured by G-MDSC isolated from 3LL and MCA-38 tumors, but no rescue was observed in those co-cultured with Mo-MDSC (Fig. 3A). Conversely, PTIO prevented the T cell suppression effect induced by Mo-MDSC in both tumor models, without having an effect in G-MDSC suppression (Fig. 3B). This suggests the specific role of PNT in the suppression induced by G-MDSC and NO in the inhibition induced by Mo-MDSC.

Role of gp91^{phox}, eNOS, and iNOS in the suppression mediated by MDSC subpopulations

To better understand the mechanisms leading to the production of PNT in G-MDSC, we used MDSC isolated from gp91^{phox} or eNOS knockout mice injected with 3LL tumors. A significant prevention in the production of PNT by G-MDSC, but not by Mo-MDSC, was found in tumor-bearing gp91^{phox} and eNOS null mice, as compared to MDSC from control mice (Fig. 4A). In addition, the decreased production of PNT in G-MDSC from gp91^{phox} or eNOS null mice correlated with a significant decrease in their ability to suppress T cell proliferation (Fig. 4B–C), suggesting the fundamental role of eNOS and gp91^{phox} in the PNT-linked suppression induced by G-MDSC.

Then, we investigated the role of iNOS in the Mo-MDSC-associated T cell suppression. Knockdown of iNOS resulted in a statistical significant decrease in the production of NO by Mo-MDSC, but it did not affect NO release in G-MDSC (Fig. 5A). Accordingly, deletion of iNOS partially impaired the ability of Mo-MDSC to suppress T cell proliferation (Fig. 5B), while it did not impact the suppressive activity and the production of PNT by G-MDSC (Fig. 5C and D). Altogether, the results suggest that iNOS plays a major role in the NO-mediated Mo-MDSC-suppression, but has little effect in regards to G-MDSC-regulatory activity.

Inhibition of MDSC subsets-suppressive pathways prevents tumor growth

We sought to investigate the effect of the deletion of gp91^{phox} and iNOS or treatments with MnTBAP on regard to tumor growth. To test this, we looked for tumors having a preferential accumulation of MDSC subsets. Increased numbers of G-MDSC were found in 3LL, B16, and EL-4 tumors, whereas Mo-MDSC preferentially accumulated in MCA-38 tumors (Fig. 6A–B). A significant prevention of 3LL tumor growth was found in gp91^{phox} knockout mice and MnTBAP-treated mice, as compared to controls (Fig. 6C–D, upper panel). Conversely, similar tumor growth kinetics were observed in 3LL cells injected into iNOS null and wild type mice (Fig. 6E). Then, we determined the effect of gp91^{phox}, iNOS, and MnTBAP on MCA-38-tumor growth, which is dominated by Mo-MDSC presence. A significant anti-tumor effect was found in iNOS null mice bearing MCA-38 cells (Fig. 6E). In contrast, deletion of gp91^{phox} and treatment with MnTBAP further enhanced tumor growth in MCA-38-bearing mice (Fig. 6C–D). Altogether the results suggest that specific deletion or inhibition of pathways associated with PNT production (gp91^{phox} and MnTBAP treatment) inhibit growth of tumors having high numbers of G-MDSC, whereas deletion of iNOS will be effective in Mo-MDSC-dominated tumors.

Discussion

The effect of MDSC in the promotion of tumor growth has been well documented during recent years. These studies suggested the fundamental role of MDSC in the induction of angiogenesis, metastasis, and most notably in the inhibition of T cell function. Among the primary mechanisms governing the inhibition of T cell responses by MDSC is the metabolism of the amino acid arginine. Previous studies showed that MDSC metabolize

arginine though arginase I and iNOS.[6] Depletion of arginine by arginase I plays a major role in the MDSC-suppression independent of cell to cell contact.[28] Furthermore, arginine metabolism in MDSC by iNOS mediated cell to cell-dependent suppression of T cells.[3] Although these pathways play a major role in the MDSC activity as a whole, it remained unclear their role in specific MDSC subsets. In this study, we show that both MDSC subpopulations rely on the activity of different NO synthases for the suppression of T cell responses. In addition, each MDSC subset uses unique effector suppressive pathways. G-MDSC blocked T cell proliferation through PNT generated through gp91^{phox} and eNOS, while iNOS-linked NO was responsible for the suppression of T cells by Mo-MDSC. Targeting these pathways severely impacted the ability each MDSC populations to inhibit T cell proliferation and IFNγ production. The results advance in the understanding of the mechanisms used by MDSC subsets to suppress immune responses. Furthermore, this study builds on previous studies[29–31] by describing the function of MDSC subpopulations in response to tumor-induced inflammation which may serve as effective targets for immune therapy.

Our results show that the global inhibition of NO synthases, using L-NMMA, prevents T cell suppression by both MDSC subpopulations. Previous findings from Dietlin et al[29] showed that MDSC produce PNT through iNOS during mycobacterium infections. We have expanded upon these findings by showing that in the tumor microenvironment the expression of eNOS is a critical player in the suppressive activity of G-MDSC by acting as a source of NO for PNT production. The promotion of PNT through eNOS may be explained by the cellular location of the active form eNOS and its close proximity to the O_2^- synthesized by gp91^{phox}.[32] In fact, deletion of gp91^{phox} or eNOS significantly impaired the production of PNT in G-MDSC. It is also possible that the expression of arginase I in G-MDSC contributes to the synthesis of PNT, as the decrease in arginine can modulate the production of NO into PNT.[10] In fact, MDSC co-expressing arginase I and iNOS displayed a higher ability to impair $CD8^+$ T cell function through the elevated production of PNT.[8,10,33,34] The mechanisms of how PNT block T cell responses have been partially identified during recent years. PNT impair the conformational flexibility of the T cell antigen receptor and its interaction with MHC by inducing nitration of T cell antigen receptor proteins in $CD8^+$ cells and the MHC in antigen presenting cells.[16,35] In addition, PNT induces apoptosis in activated T cells.[18] This suppression requires the production of IL-13 and IFN-γ[33,36,37] and signaling through STAT1 transcription factor[10].

The results also suggest the role of the iNOS-linked NO in the suppression induced by Mo-MDSC. Production of NO has three primary effects. First, the generation of NO, which directly inhibits T cell function by mechanisms that are not fully understood. Second, NO synthesis contributes to the depletion of arginine leading to amino acid starvation-induced suppression. Third, NO readily reacts with O_2^- to produce PNT. Our results show a partial inhibition of Mo-MDSC suppressive activity by NO scavenger PTIO, but not by PNT scavenger MnTBAP, suggesting the major direct effect of NO in Mo-MDSC-induced suppression. However, it is unclear why Mo-MDSC exclusively use iNOS as a suppressive mechanism for the release NO rather than the starvation of arginine or the production of PNT. This could be explained by the decreased expression in Mo-MDSC of enzymes associated with ROS production such as gp91^{phox} and additional enzymes metabolizing arginine such as arginase I. Also, the fact that Mo-MDSC are less suppressive in a cell-cell basis, as compared to G-MDSC, suggest that the NO-inhibitory mechanism is less effective in reaching T cell suppression as compared to the PNT production. Interestingly, we found that the responses of tumors to inhibition of pathways associated with PNT or NO production will depend on the accumulation of specific MDSC subsets. Deletion of gp91^{phox} and MnTBAP treatment induced anti-tumor effects in 3LL tumors, which had more G-MDSC, whereas iNOS knockdown inhibited MCA-38 tumor growth, which preferentially

accumulated Mo-MDSC. However, a broad suppression of both MDSC subsets could be achieved after the common pharmacological inhibition of NO synthases (Fig. 1E).

Interestingly, previous studies, including our own[8,38,39], suggested that MDSC were not affected by treatment with the NOS inhibitor L-NMMA and were more susceptible to treatment with an arginase I inhibitor. However, most of these studies were performed using transwell assays which exclude cell-to-cell contact mechanisms. Our current study focuses on the mechanisms leading to T cell inhibition incurred upon direct contact with MDSC. Furthermore, a significant portion of the previously published findings regarding MDSC subpopulations were performed using cells isolated from the spleens of tumor bearing mice as opposed to our present approach which utilizes MDSC isolated from the tumors. This distinction is extremely important as it advances our knowledge of different MDSC suppressive activities based on location which may also explain some discrepancies between published studies. In particular, several studies often implicate Mo-MDSC as a more suppressive subpopulation[30,31,40–42]. While this may be true for MDSC populations from the spleens of tumor bearing mice or MDSC generated *in vitro*, we find at the tumor site of several tumor models that G-MDSC are more suppressive as compared to Mo-MDSC. This point is critical for our understanding of MDSC as it highlights the relevance of the tumor microenvironment and its potential effects on specific MDSC subpopulations.

An important question is what is the role of Mo-MDSC when G-MDSC are clearly more efficient in regulating anti-tumor responses? A recent publication from Gabrilovich group[43] indicated that Mo-MDSC accumulate at the tumor site and then differentiate into G-MDSC. Their data suggests that a large subset of Mo-MDSC down regulate Rb1 and subsequently take on the functional and morphological characteristics of G-MDSC. In the context our study, the conversion of Mo-MDSC to G-MDSC would indicate the conversion of a less suppressive population producing NO to a highly suppressive PNT-producing population. Hence, we may hypothesize that recruitment of Mo-MDSC to the tumor site functions not only as a T cell inhibitory mechanism but also acts as reinforcement to maintain a steady population of hyper-suppressive G-MDSC in the tumor microenvironment.

The role of PNT and NO as a major effector suppressive mechanism in human MDSC is still undetermined. Human G-MDSC display the phenotype $CD11b^{+}$ $CD33^{+}CD14^{NEG}$ $CD15^{+}$ $CD66b^{+}$, while Mo-MDSC are $CD11b^{+}CD33^{+}$ $CD14^{+}$ MHC Class $II^{Low\text{-}NEG}CD15^{NEG}$.[7,44,45] Our previous studies suggested the production of arginase and PNT in a population of G-MDSC from renal cell carcinoma patients.[7] Therefore, it is highly possible that the same mechanisms identified in this study, translate into human MDSC subpopulations. Characterization of the pathways by which human MDSC suppress T cell responses will enable the generation of therapies to specifically target MDSC in diseases where specific MDSC subsets are predominant.

In summary, this study identified the independent NO-related effector mechanisms by which MDSC impairs T cell responses. It could represent the foundation for the development of specific therapies targeting particular subpopulations of MDSC in tumors and other diseases characterized by the accumulation of MDSC subsets and T cell dysfunction.

Supplementary Material

Refer to Web version on PubMed Central for supplementary material.

Acknowledgments

We thank Jonna Ellis for her administrative assistance in this study.

Financial support: This work was supported in part by National Institutes of Health (NIH) grant P20GM103501 subproject #3 to P.C.R., NIH-R21CA162133 to P.C.R., and Hope on wheels Hyundai grant to P.C.R. and M.F.

Abbreviations

MDSC	Myeloid-derived suppressor cells
NO	nitric oxide
PNT	peroxynitrites
NOS	nitric oxide synthase
O_2^-	superoxide anion

Reference List

1. Coussens LM, Zitvogel L, Palucka AK. Neutralizing tumor-promoting chronic inflammation: a magic bullet? Science. 2013; 339:286–291. [PubMed: 23329041]
2. Gabrilovich DI, Ostrand-Rosenberg S, Bronte V. Coordinated regulation of myeloid cells by tumours. Nat Rev Immunol. 2012; 12:253–268. [PubMed: 22437938]
3. Raber P, Ochoa AC, Rodriguez PC. Metabolism of L-arginine by myeloid-derived suppressor cells in cancer: mechanisms of T cell suppression and therapeutic perspectives. Immunol Invest. 2012; 41:614–634. [PubMed: 23017138]
4. Gabrilovich DI, Nagaraj S. Myeloid-derived suppressor cells as regulators of the immune system. Nat Rev Immunol. 2009; 9:162–174. [PubMed: 19197294]
5. Greten TF, Manns MP, Korangy F. Myeloid derived suppressor cells in human diseases. Int Immunopharmacol. 2011; 11:802–807. [PubMed: 21237299]
6. Gabrilovich DI, Bronte V, Chen SH, Colombo MP, Ochoa A, Ostrand-Rosenberg S, Schreiber H. The terminology issue for myeloid-derived suppressor cells. Cancer Res. 2007; 67:425. [PubMed: 17210725]
7. Rodriguez PC, Ernstoff MS, Hernandez C, Atkins M, Zabaleta J, Sierra R, Ochoa AC. Arginase I-producing myeloid-derived suppressor cells in renal cell carcinoma are a subpopulation of activated granulocytes. Cancer Res. 2009; 69:1553–1560. [PubMed: 19201693]
8. Rodriguez PC, Quiceno DG, Zabaleta J, Ortiz B, Zea AH, Piazuelo MB, Delgado A, Correa P, Brayer J, Sotomayor EM, Antonia S, Ochoa JB, et al. Arginase I production in the tumor microenvironment by mature myeloid cells inhibits T-cell receptor expression and antigen-specific T-cell responses. Cancer Res. 2004; 64:5839–5849. [PubMed: 15313928]
9. Srivastava MK, Sinha P, Clements VK, Rodriguez P, Ostrand-Rosenberg S. Myeloid-derived suppressor cells inhibit T-cell activation by depleting cystine and cysteine. Cancer Res. 2010; 70:68–77. [PubMed: 20028852]
10. Kusmartsev S, Gabrilovich DI. STAT1 signaling regulates tumor-associated macrophage-mediated T cell deletion. J Immunol. 2005; 174:4880–4891. [PubMed: 15814715]
11. Jayaraman P, Parikh F, Lopez-Rivera E, Hailemichael Y, Clark A, Ma G, Cannan D, Ramacher M, Kato M, Overwijk WW, Chen SH, Umansky VY, et al. Tumor-expressed inducible nitric oxide synthase controls induction of functional myeloid-derived suppressor cells through modulation of vascular endothelial growth factor release. J Immunol. 2012; 188:5365–5376. [PubMed: 22529296]
12. Kusmartsev S, Nefedova Y, Yoder D, Gabrilovich DI. Antigen-specific inhibition of CD8+ T cell response by immature myeloid cells in cancer is mediated by reactive oxygen species. J Immunol. 2004; 172:989–999. [PubMed: 14707072]
13. Corzo CA, Cotter MJ, Cheng P, Cheng F, Kusmartsev S, Sotomayor E, Padhya T, McCaffrey TV, McCaffrey JC, Gabrilovich DI. Mechanism regulating reactive oxygen species in tumor-induced myeloid-derived suppressor cells. J Immunol. 2009; 182:5693–5701. [PubMed: 19380816]

14. Lu T, Ramakrishnan R, Altiok S, Youn JI, Cheng P, Celis E, Pisarev V, Sherman S, Sporn MB, Gabrilovich D. Tumor-infiltrating myeloid cells induce tumor cell resistance to cytotoxic T cells in mice. J Clin Invest. 2011; 121:4015–4029. [PubMed: 21911941]
15. Bronte V, Apolloni E, Cabrelle A, Ronca R, Serafini P, Zamboni P, Restifo NP, Zanovello P. Identification of a CD11b(+)/Gr-1(+)/CD31(+) myeloid progenitor capable of activating or suppressing CD8(+) T cells. Blood. 2000; 96:3838–3846. [PubMed: 11090068]
16. Nagaraj S, Gupta K, Pisarev V, Kinarsky L, Sherman S, Kang L, Herber DL, Schneck J, Gabrilovich DI. Altered recognition of antigen is a mechanism of CD8+ T cell tolerance in cancer. Nat Med. 2007; 13:828–835. [PubMed: 17603493]
17. Yang GY, Taboada S, Liao J. Induced nitric oxide synthase as a major player in the oncogenic transformation of inflamed tissue. Methods Mol Biol. 2009; 512:119–156. [PubMed: 19347276]
18. Kasic T, Colombo P, Soldani C, Wang CM, Miranda E, Roncalli M, Bronte V, Viola A. Modulation of human T-cell functions by reactive nitrogen species. Eur J Immunol. 2011; 41:1843–1849. [PubMed: 21480210]
19. Hess DT, Stamler JS. Regulation by S-nitrosylation of protein post-translational modification. J Biol Chem. 2012; 287:4411–4418. [PubMed: 22147701]
20. Molon B, Ugel S, Del PF, Soldani C, Zilio S, Avella D, De PA, Mauri P, Monegal A, Rescigno M, Savino B, Colombo P, et al. Chemokine nitration prevents intratumoral infiltration of antigen-specific T cells. J Exp Med. 2011; 208:1949–1962. [PubMed: 21930770]
21. Brito C, Naviliat M, Tiscornia AC, Vuillier F, Gualco G, Dighiero G, Radi R, Cayota AM. Peroxynitrite inhibits T lymphocyte activation and proliferation by promoting impairment of tyrosine phosphorylation and peroxynitrite-driven apoptotic death. J Immunol. 1999; 162:3356–3366. [PubMed: 10092790]
22. Bronte V, Kasic T, Gri G, Gallana K, Borsellino G, Marigo I, Battistini L, Iafrate M, Prayer-Galetti T, Pagano F, Viola A. Boosting antitumor responses of T lymphocytes infiltrating human prostate cancers. J Exp Med. 2005; 201:1257–1268. [PubMed: 15824085]
23. De SC, Serafini P, Marigo I, Dolcetti L, Bolla M, Del SP, Melani C, Guiducci C, Colombo MP, Iezzi M, Musiani P, Zanovello P, et al. Nitroaspirin corrects immune dysfunction in tumor-bearing hosts and promotes tumor eradication by cancer vaccination. Proc Natl Acad Sci U S A. 2005; 102:4185–4190. [PubMed: 15753302]
24. Norell H, Martins da PT, Lesher A, Kaur N, Mehrotra M, Naga OS, Spivey N, Olafimihan S, Chakraborty NG, Voelkel-Johnson C, Nishimura MI, Mukherji B, et al. Inhibition of superoxide generation upon T-cell receptor engagement rescues Mart-1(27–35)-reactive T cells from activation-induced cell death. Cancer Res. 2009; 69:6282–6289. [PubMed: 19638595]
25. Rodriguez PC, Hernandez CP, Quiceno D, Dubinett SM, Zabaleta J, Ochoa JB, Gilbert J, Ochoa AC. Arginase I in myeloid suppressor cells is induced by COX-2 in lung carcinoma. J Exp Med. 2005; 202:931–939. [PubMed: 16186186]
26. Batinic-Haberle I, Cuzzocrea S, Reboucas JS, Ferrer-Sueta G, Mazzon E, Di PR, Radi R, Spasojevic I, Benov L, Salvemini D. Pure MnTBAP selectively scavenges peroxynitrite over superoxide: comparison of pure and commercial MnTBAP samples to MnTE-2-PyP in two models of oxidative stress injury, an SOD-specific Escherichia coli model and carrageenan-induced pleurisy. Free Radic Biol Med. 2009; 46:192–201. [PubMed: 19007878]
27. Goldstein S, Russo A, Samuni A. Reactions of PTIO and carboxy-PTIO with *NO, *NO2, and O2-*. J Biol Chem. 2003; 278:50949–50955. [PubMed: 12954619]
28. Rodriguez PC, Ochoa AC. Arginine regulation by myeloid derived suppressor cells and tolerance in cancer: mechanisms and therapeutic perspectives. Immunol Rev. 2008; 222:180–191. [PubMed: 18364002]
29. Dietlin TA, Hofman FM, Lund BT, Gilmore W, Stohlman SA, van d V. Mycobacteria-induced Gr-1+ subsets from distinct myeloid lineages have opposite effects on T cell expansion. J Leukoc Biol. 2007; 81:1205–1212. [PubMed: 17307863]
30. Movahedi K, Guilliams M, Van den BJ, Van den BR, Gysemans C, Beschin A, De BP, Van Ginderachter JA. Identification of discrete tumor-induced myeloid-derived suppressor cell subpopulations with distinct T cell-suppressive activity. Blood. 2008; 111:4233–4244. [PubMed: 18272812]

31. Youn JI, Nagaraj S, Collazo M, Gabrilovich DI. Subsets of myeloid-derived suppressor cells in tumor-bearing mice. J Immunol. 2008; 181:5791–5802. [PubMed: 18832739]
32. Rafikov R, Fonseca FV, Kumar S, Pardo D, Darragh C, Elms S, Fulton D, Black SM. eNOS activation and NO function: structural motifs responsible for the posttranslational control of endothelial nitric oxide synthase activity. J Endocrinol. 2011; 210:271–284. [PubMed: 21642378]
33. Sinha P, Clements VK, Ostrand-Rosenberg S. Reduction of myeloid-derived suppressor cells and induction of M1 macrophages facilitate the rejection of established metastatic disease. J Immunol. 2005; 174:636–645. [PubMed: 15634881]
34. Van Ginderachter JA, Meerschaut S, Liu Y, Brys L, De GK, Hassanzadeh GG, Raes G, De BP. Peroxisome proliferator-activated receptor gamma (PPARgamma) ligands reverse CTL suppression by alternatively activated (M2) macrophages in cancer. Blood. 2006; 108:525–535. [PubMed: 16527895]
35. Li F, Lu J, Ma X. Metabolomic screening and identification of the bioactivation pathways of ritonavir. Chem Res Toxicol. 2011; 24:2109–2114. [PubMed: 22040299]
36. Sinha P, Clements VK, Ostrand-Rosenberg S. Interleukin-13-regulated M2 macrophages in combination with myeloid suppressor cells block immune surveillance against metastasis. Cancer Res. 2005; 65:11743–11751. [PubMed: 16357187]
37. Gallina G, Dolcetti L, Serafini P, De SC, Marigo I, Colombo MP, Basso G, Brombacher F, Borrello I, Zanovello P, Bicciato S, Bronte V. Tumors induce a subset of inflammatory monocytes with immunosuppressive activity on CD8+ T cells. J Clin Invest. 2006; 116:2777–2790. [PubMed: 17016559]
38. Bunt SK, Yang L, Sinha P, Clements VK, Leips J, Ostrand-Rosenberg S. Reduced inflammation in the tumor microenvironment delays the accumulation of myeloid-derived suppressor cells and limits tumor progression. Cancer Res. 2007; 67:10019–10026. [PubMed: 17942936]
39. Sinha P, Clements VK, Bunt SK, Albelda SM, Ostrand-Rosenberg S. Cross-talk between myeloid-derived suppressor cells and macrophages subverts tumor immunity toward a type 2 response. J Immunol. 2007; 179:977–983. [PubMed: 17617589]
40. Haile LA, Gamrekelashvili J, Manns MP, Korangy F, Greten TF. CD49d is a new marker for distinct myeloid-derived suppressor cell subpopulations in mice. J Immunol. 2010; 185:203–210. [PubMed: 20525890]
41. Highfill SL, Rodriguez PC, Zhou Q, Goetz CA, Koehn BH, Veenstra R, Taylor PA, Panoskaltsis-Mortari A, Serody JS, Munn DH, Tolar J, Ochoa AC, et al. Bone marrow myeloid-derived suppressor cells (MDSCs) inhibit graft-versus-host disease (GVHD) via an arginase-1-dependent mechanism that is up-regulated by interleukin-13. Blood. 2010; 116:5738–5747. [PubMed: 20807889]
42. Marigo I, Bosio E, Solito S, Mesa C, Fernandez A, Dolcetti L, Ugel S, Sonda N, Bicciato S, Falisi E, Calabrese F, Basso G, et al. Tumor-induced tolerance and immune suppression depend on the C/EBPbeta transcription factor. Immunity. 2010; 32:790–802. [PubMed: 20605485]
43. Youn JI, Kumar V, Collazo M, Nefedova Y, Condamine T, Cheng P, Villagra A, Antonia S, McCaffrey JC, Fishman M, Sarnaik A, Horna P, et al. Epigenetic silencing of retinoblastoma gene regulates pathologic differentiation of myeloid cells in cancer. Nat Immunol. 2013; 14:211–220. [PubMed: 23354483]
44. Zea AH, Rodriguez PC, Atkins MB, Hernandez C, Signoretti S, Zabaleta J, McDermott D, Quiceno D, Youmans A, O'Neill A, Mier J, Ochoa AC. Arginase-producing myeloid suppressor cells in renal cell carcinoma patients: a mechanism of tumor evasion. Cancer Res. 2005; 65:3044–3048. [PubMed: 15833831]
45. Solito S, Falisi E, az-Montero CM, Doni A, Pinton L, Rosato A, Francescato S, Basso G, Zanovello P, Onicescu G, Garrett-Mayer E, Montero AJ, et al. A human promyelocytic-like population is responsible for the immune suppression mediated by myeloid-derived suppressor cells. Blood. 2011; 118:2254–2265. [PubMed: 21734236]

Novelty and Impact statements

Our study describes the independent suppressive pathways by which tumor-infiltrating MDSC-subpopulations impair T cell function in tumor bearing host. In addition, our results show for the first time the differential effector role of nitric oxide-mediated pathways in the T cell suppression induced by MDSC subsets.

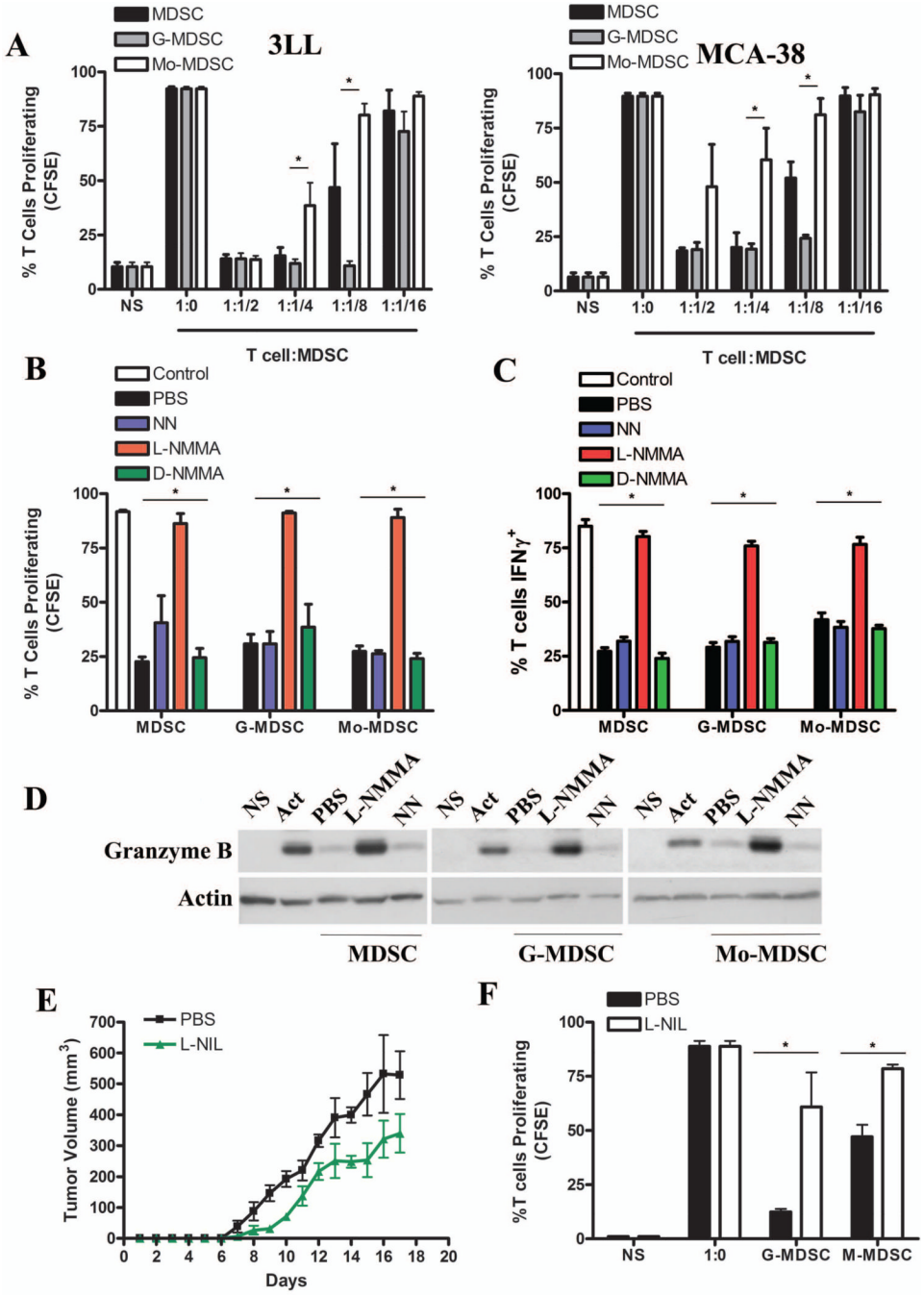

Figure 1. Suppression of T cell proliferation by MDSC subpopulations depends on nitric oxide synthases

A. CFSE labeled $CD3^+$ T cells were co-cultured at different ratios with MDSC, G-MDSC, and Mo-MDSC positively isolated from 3LL or MCA-38 tumors. T cell proliferation was assessed by flow cytometry 72 hours later. NS indicates non-stimulated T cells, while 1:0 indicates T cells activated with anti-CD3/CD28 and cultured alone. **B**. T cells co-cultured with MDSC, G-MDSC, and Mo-MDSC at a 1:1/2 ratio were treated with NN (200 μM), L-NMMA (500 μM), and D-NMMA(500 μM). Then, proliferation was tested by flow cytometry. **C**. T cells negatively selected from **B** were tested for IFNγ production by intracellular staining. Values are from 3 similar experiments. **D.** A representative experiment

from 3 showing western blot for granzyme B expression in T cells previously co-cultured with MDSC populations in the presence of NN and L-NMMA. **E**. Mice bearing 3LL tumors were treated daily with PBS (n=10) or L-NIL (20 mg/kg) (n=10), and tumor burden was assessed. **F**. G-MDSC and Mo-MDSC positively isolated from the tumors of each treatment group were co-cultured with naïve $CD3^+$ T cells at a ratio of 1:1/4 and suppression was determined as described above. Values are from 3 similar experiments. * $p < 0.05$

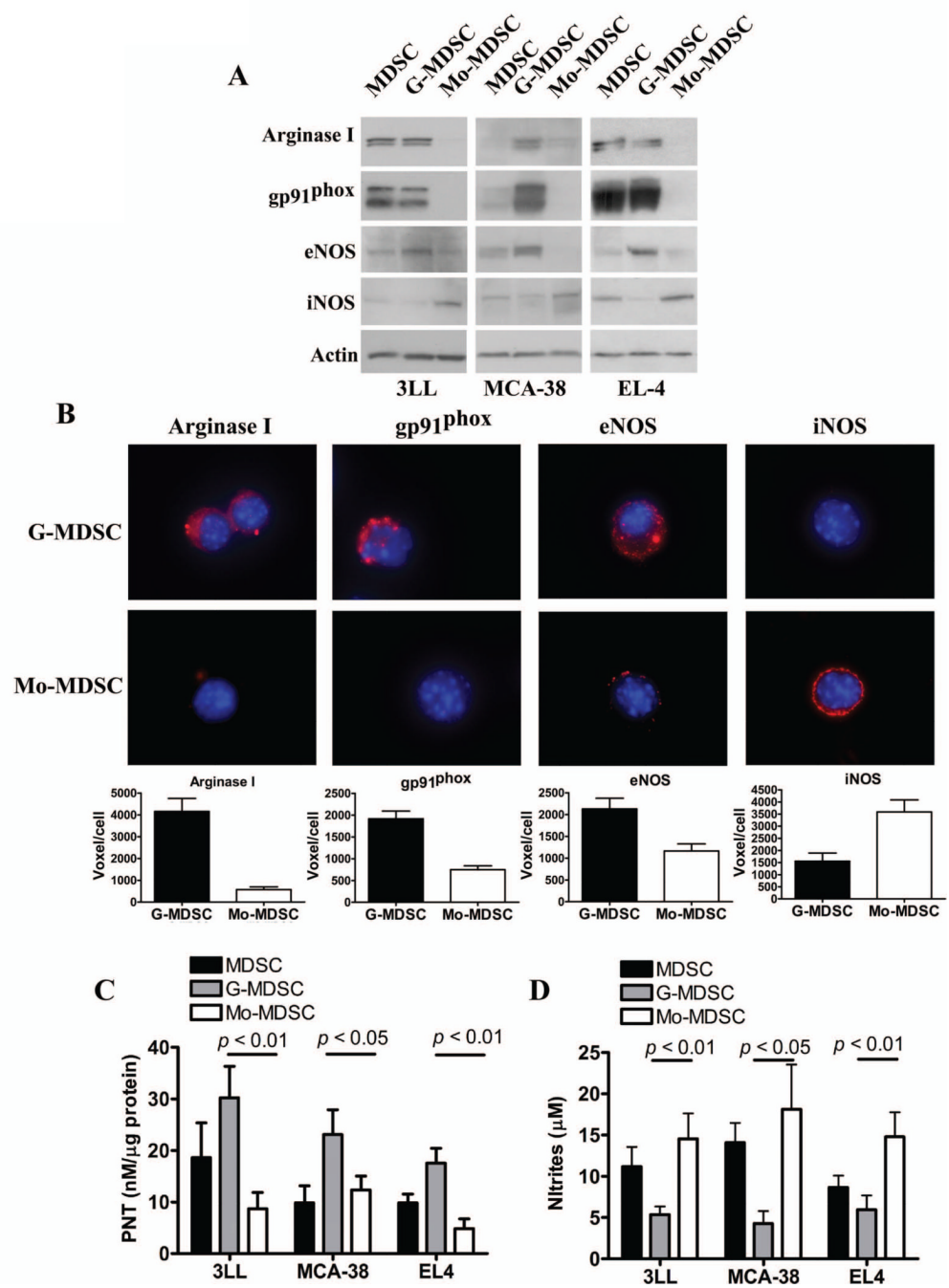

Figure 2. Differential expression of suppressive pathways in tumor-infiltrating MDSC subpopulations

A. Expression of arginase I, gp91^{phox}, eNOS, and iNOS in MDSC, G-MDSC, and Mo-MDSC isolated from 3LL, MCA-38, and EL-4 tumors. Values are a representative experiment from 5 individual mice. **B**. The same panel of suppressive enzymes was determined by immuno cytology and the voxel per cell determined, as described in the methods. **C**. Nitrotyrosine ELISA of whole cell extracts from tumor isolated MDSC subpopulations was used to quantify PNT production (n=10). **D**. NO production by MDSC subsets was determined using Griess reagent (n=10).

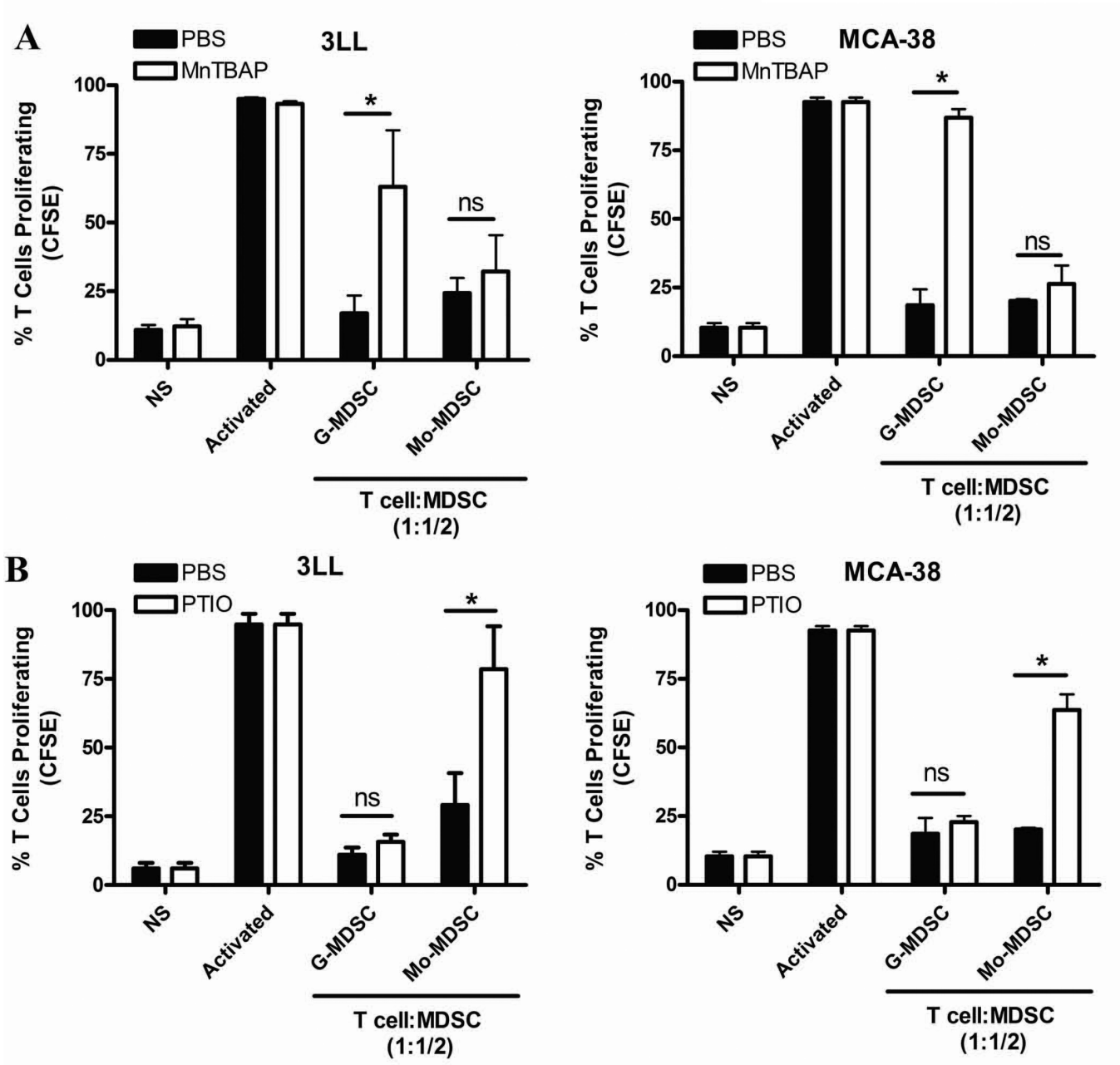

Figure 3. MDSC subpopulations inhibit T cell proliferation through independent nitric-oxide related pathways

A. Co-cultures of activated CFSE-labeled T cells and G-MDSC subpopulations (ratio 1:1/2) were established in the presence of PNT scavenger MnTBAP (100 μM). Then, T cell proliferation was evaluated 72 hours later. B. Similar to experiment **A**, T cells: MDSC subsets (ratio 1:1/2) were cultured in the presence of PTIO (100 μM) and T cell proliferation tested after 72 hours. The experiments were repeated a minimum of 3 times obtaining similar results. * $p < 0.01$; Non-statistical significant differences (ns): $p > 0.05$

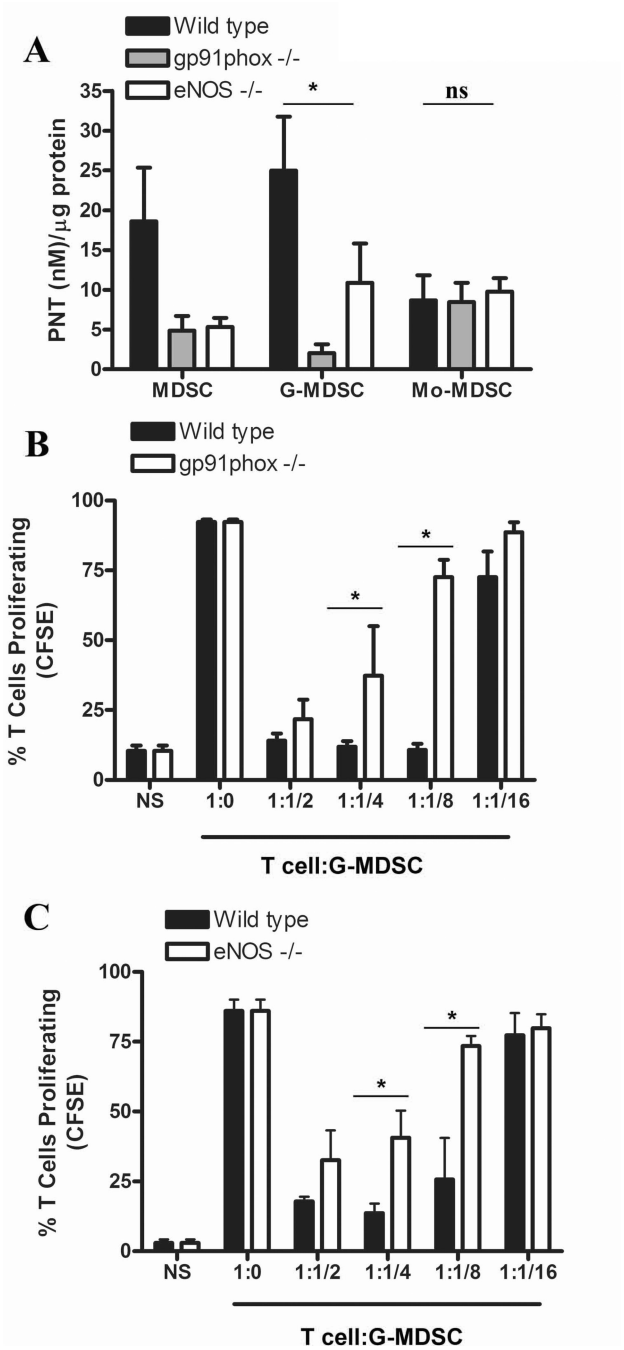

Figure 4. G-MDSC suppress T cells by production of PNT derived from gp91^{phox} and eNOS

A. PNT levels were evaluated by nitrotyrosine ELISA from whole cell extracts of MDSC subpopulations isolated from wild-type, eNOS −/−, and gp91^{phox}−/− mice bearing 3LL tumors for 17 days (n=10). **B–C**. G-MDSC from wild-type, gp91^{phox}−/− (**B**), or eNOS−/− (**C**) mice bearing 3LL tumors were co-cultured with CFSE labeled T cells to determine the suppressive capacity. The experiment was repeated a minimum of 3 times using independent tumor bearing mice obtaining similar results. * $p < 0.01$, Non-statistical significant differences (ns): $p > 0.05$

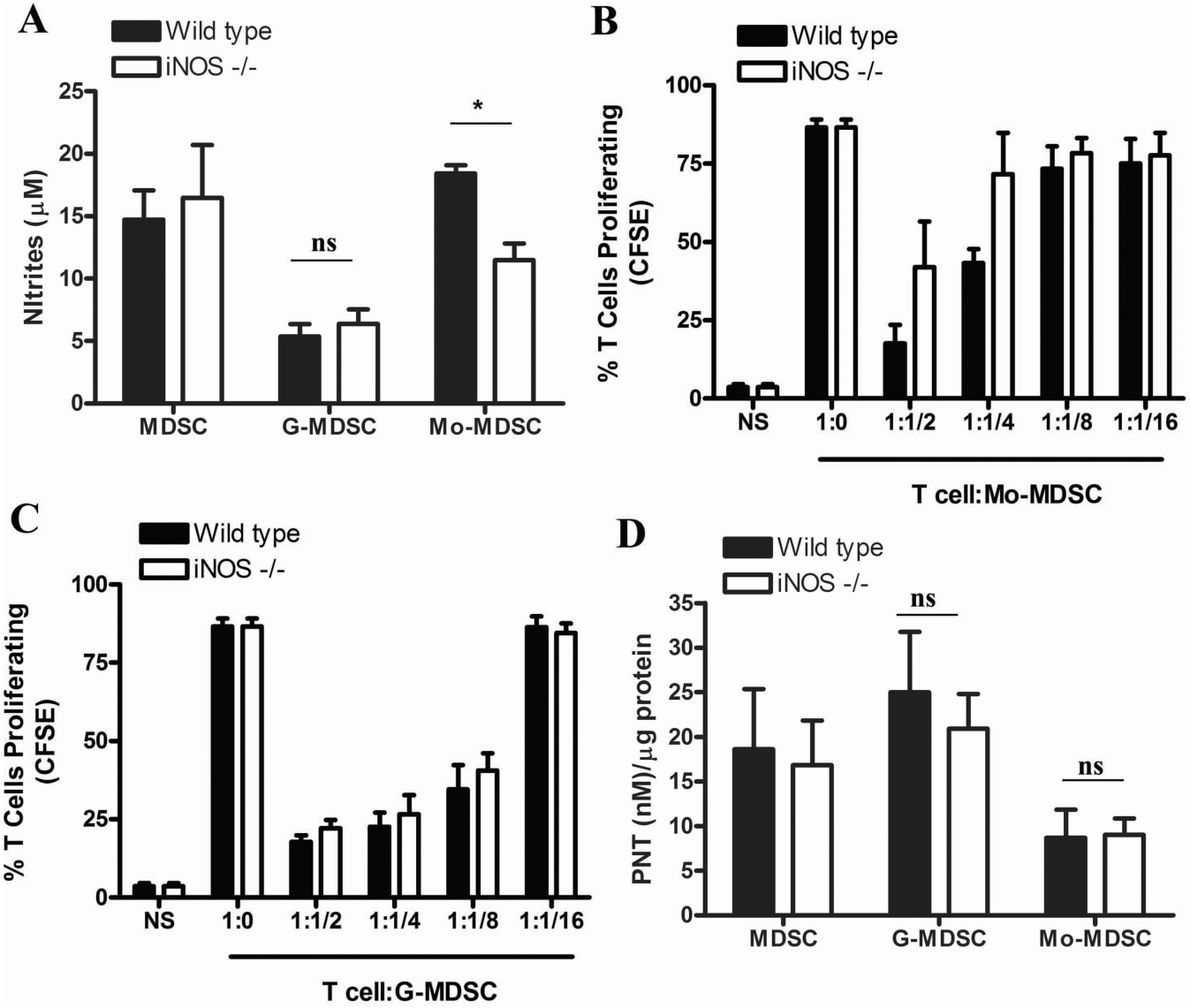

Figure 5. Mo-MDSC suppress T cell proliferation by NO production derived from iNOS

A. Comparison of nitrities from G-MDSC and Mo-MDSC isolated from wild-type and iNOS −/− mice bearing 3LL tumors for 17 days (n=10). **B–C**. Mo-MDSC (**B**) and G-MDSC (**C**) were collected from wild-type and iNOS−/− mice bearing 3LL tumors and co-cultured with CFSE labeled T cells. Proliferation of T cells was established 72 hours later. The experiment was repeated a minimum of 3 times obtaining similar results. **D**. PNT production from each population was analyzed by nitrotyrosine ELISA (n=9). * $p < 0.01$; Non-statistical significant differences (ns): $p > 0.05$

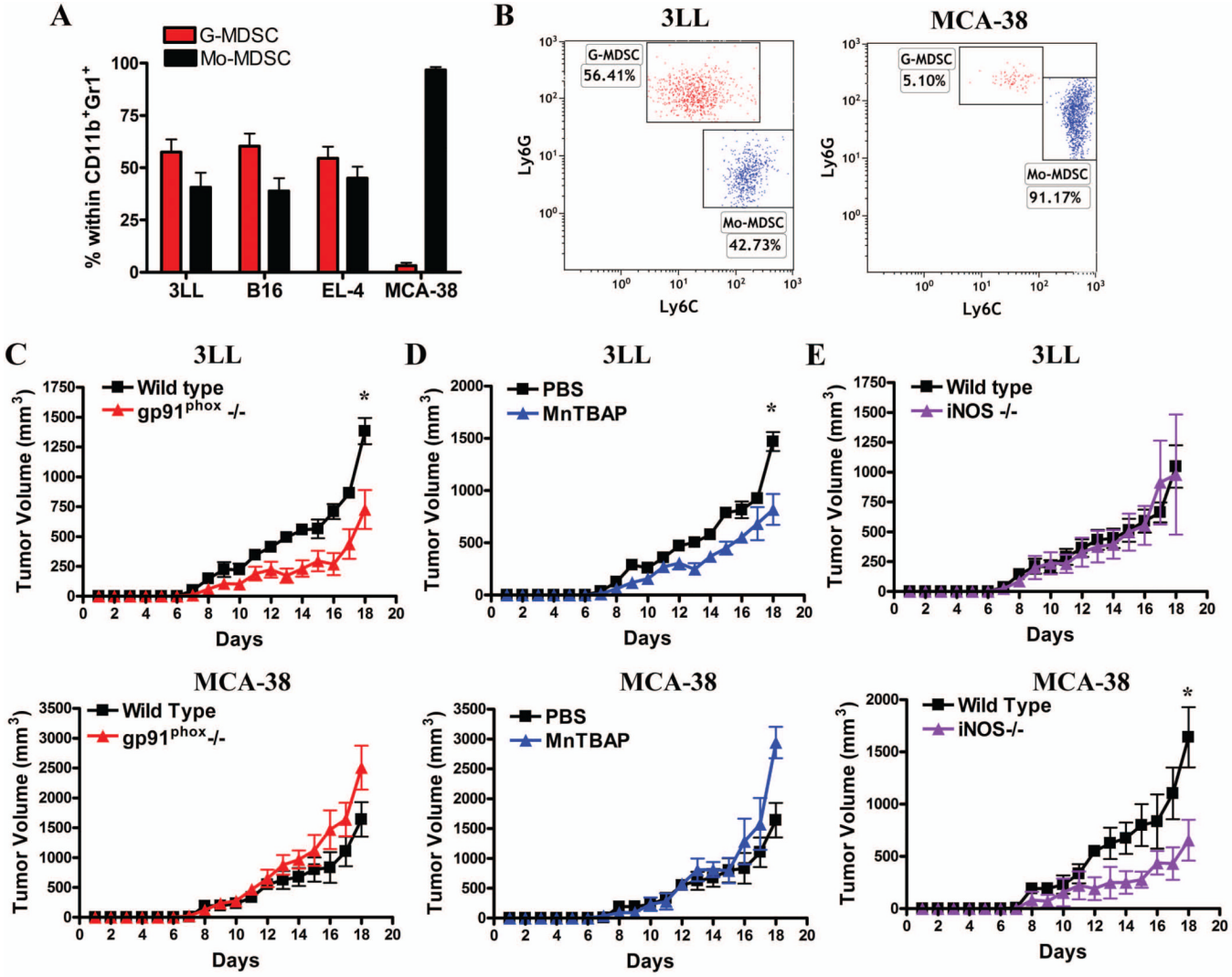

Figure 6. Targeting MDSC subset-associated suppressive pathways blocks tumor growth

A. Accumulation of G-MDSC ($CD11b^{+}Ly6C^{LOW}$ $Ly6G^{HIGH}$) and Mo-MDSC ($CD11b^{+}$ $Ly6C^{HIGH}$ $Ly6G^{NEG-LOW}$) in tumors from mice injected with 3LL, B16, EL-4, or MCA-38 tumors. **B**. A representative experiment showing higher numbers of G-MDSC in 3LL tumors (n=10) and the preferential accumulation of Mo-MDSC in MCA-38 tumors (n=10). **C**. 3LL (upper panel) or MCA-38 (lower panel) cells were subcutaneously injected into wild-type and $gp91^{phox}$−/− mice and tumor volume measured daily (n=10). **D**. To determine the role of PNT production on tumor burden, mice were subcutaneously injected with 3LL or MCA-38 cells and treated daily with the PNT scanvenger (MnTBAP) or PBS control (n=10). **E**. iNOS−/− mice were injected with 3LL or MCA-38 cells and their growth compared with wild type mice (n=10). * $p < 0.01$, Non-statistical significant differences (ns): $p > 0.05$